



## Electrospun magnetic nanofibre mats – A new bondable biomaterial using remotely activated magnetic heating



Yi Zhong<sup>a,e</sup>, Victor Leung<sup>a</sup>, Lynn Yuqin Wan<sup>a</sup>, Silvio Dutz<sup>c,d</sup>, Frank K. Ko<sup>a</sup>, Urs O. Häfeli<sup>b,\*</sup>

<sup>a</sup> Department of Materials Engineering, University of British Columbia, Vancouver, Canada

<sup>b</sup> Faculty of Pharmaceutical Sciences, University of British Columbia, Vancouver, Canada

<sup>c</sup> Institut für Biomedizinische Technik und Informatik, Technische Universität Ilmenau, Germany

<sup>d</sup> Department of Nano Biophotonics, Leibniz Institute of Photonic Technology, Jena, Germany

<sup>e</sup> Key Laboratory of Science & Technology of Eco-Textile, Ministry of Education, College of Chemistry, Chemical Engineering and Biotechnology, Donghua University, Shanghai, China

### ARTICLE INFO

#### Article history:

Received 15 July 2014

Received in revised form

28 September 2014

Accepted 28 September 2014

Available online 6 October 2014

#### Keywords:

Solvothermal

Hydrophilic Fe<sub>3</sub>O<sub>4</sub>

Magnetic nanofibre

Hyperthermia

Electrospinning

Polymer bonding

Heat sealing

### ABSTRACT

A solvothermal process was adopted to produce hydrophilic magnetite (Fe<sub>3</sub>O<sub>4</sub>) nanoparticles which were subsequently emulsified with a chloroform/methanol (70/30 v/v) solution of poly(caprolactone) (PCL) and then electrospun into a 0.2 mm thick PCL mat. The magnetic heating of the mats at a field amplitude of 25 kA/m and frequency of 400 kHz exhibited promising efficiency for magnetic hyperthermia, with a specific absorption rate of about 40 W/g for the magnetic mat. The produced heat was used to melt the magnetic mat onto the surrounding non-magnetic polymer mat from within, without destroying the nanostructure of the non-magnetic polymer more than 0.5 mm away. Magnetic nanofibre mats might thus be useful for internal heat sealing applications, and potentially also for thermotherapy.

© 2014 Elsevier B.V. All rights reserved.

### 1. Introduction

Exposure of magnetic nanoparticles to alternating magnetic fields leads to a temperature increase in the particles due to magnetization reversal losses [1,2]. This effect finds application in magnetic particle hyperthermia, where the particles are administered to tumor tissue and heated up magnetically. The ensuing temperature increase results in tumor cell death seen as shrinkage of tumor volume or a complete regression of the tumor [3,4]. Recent state of the art of this promising minimal invasive tumor therapy is given in several comprehensive review articles [5–8].

For clinical applications, the magnetic particles must be biocompatible, non-toxic, and non-immunogenic [9]. Several studies reported a vast range of magnetic materials that can be applied in biotechnology. Iron oxide particles represented by magnetite (Fe<sub>3</sub>O<sub>4</sub>) and maghemite (γ-Fe<sub>2</sub>O<sub>3</sub>) are considered promising candidates because they are biocompatible, have high saturation magnetization and stable magnetic response. Relatively easy to functionalize with polymers or functional groups, they also have

higher resistance to oxidation than other metal compounds [10,11].

For magnetic hyperthermia applications, the need to control the particle size is further required in order to optimize the energy transfer to the biologic tissue. High polydispersity of the nanoparticles' size diminishes the magnetic heating effectiveness [12]. Due to the high surface area to volume ratio, and the strong dipole–dipole interactions and van der Waals attractive forces, magnetic nanoparticles tend to agglomerate and form large clusters resulting in increased particle size [13]. Surface coating of the nanoparticles prevents aggregation and may provide colloidal stability by steric and/or electrostatic repulsion [14].

One method of magnetic nanoparticle immobilization is to incorporate them into an appropriate solid nanocarrier, such as nanofibres [15]. Nanofibres with their high surface area are attractive vehicles to carry and deliver thermal and electromagnetic properties. The most effective method to prepare them is by electrospinning, producing nanosized fibers [16]. The process has been used to incorporate many different functional elements such as drugs and carbon nanotubes into the fibers, and to form scaffolds for tissue engineering and technical applications [17,18].

Polymeric materials can be used as a matrix to encapsulate/bind the nanoparticles to facilitate handling of the nanoparticles.

\* Corresponding author. Fax: +1 604 822 3035.

E-mail addresses: [frank.ko@ubc.ca](mailto:frank.ko@ubc.ca) (F.K. Ko), [urs.hafeli@ubc.ca](mailto:urs.hafeli@ubc.ca) (U.O. Häfeli).

By fabrication of the magnetite/polymer matrix composite in nanofibre form a highly flexible and conformable magnetic substrate with ultrahigh surface area is formed. Magnetic heating can be induced when magnetite nanoparticles are placed in an alternating magnetic field under appropriate combination of field strength and frequencies. The heat generation is proportional to the amount of magnetite. Magnetic particles embedded within this fiber matrix show similar magnetic behavior regarding their heating potential as particles administered to tissue where particles are immobilized on cellular structures [19].

In this study we report the design and fabrication of magnetic nanofibre mats wherein the polymeric fibers of suitable melting point could be melted by remote heating induced in an alternating electro-magnetic field. Such a method would be useful to precisely supply heat energy in order to bond layers consisting of different (polymeric) materials in places inside the body where access is limited. Furthermore, magnetic nanofibre mats might serve as scaffolds which have a mechanical function during/after surgery, and might thereafter also be heated magnetically to release drugs or perform mild hyperthermia.

## 2. Materials and methods

### 2.1. Materials

Iron(III)chloride ( $\text{FeCl}_3$ ), sodium acetate, ethylene glycol and poly( $\epsilon$ -caprolactone) (PCL) (MW 65 kDa) were purchased from

Sigma-Aldrich (Oakville, ON). The solvents chloroform and methanol were purchased in ACS reagent grade from Fisher Scientific (Ottawa, ON).

### 2.2. Methods

**Preparation of hydrophilic  $\text{Fe}_3\text{O}_4$  nanoparticles:** Hydrophilic  $\text{Fe}_3\text{O}_4$  nanoparticles (MNPs) were synthesized using the solvothermal method similar to that used by Deng et al. [20].  $\text{FeCl}_3$  (1.46 g, 9 mmol) and sodium acetate (7.02 g) were added into ethylene glycol (30 mL) to obtain a homogeneous mixture, which was subsequently sealed and heated in a 50 mL teflon-lined stainless-steel autoclave (YH-50, Shanghai, China). After maintaining the temperature at 200 °C for 8 h, the sealed autoclave was cooled down to room temperature at a cooling-rate of 1 °C per minute. The resulting product was washed several times with distilled water and methanol, before freeze-drying for 8 h in a Console Freeze Dry System (FreeZone Plus 2.5, Labconco, USA).

**Preparation of nanofibre mats:** The polymer and up to 33 wt% MNPs in  $\text{CHCl}_3/\text{CH}_3\text{OH}$  (70/30 v/v) were electrospun from a 10 wt% suspension through a 25 gauge needle (inner diameter 0.51 mm) to produce a 0.2 mm thick mat (schematically shown in Fig. 1). The electrospinning distance was 18 cm, the pump speed 0.07 mL/min and the applied voltage 25 kV. To prepare the non-magnetic mats, a 15 wt% PCL solution without magnetic nanoparticles was used to produce a 1.0 mm thick mat, while all other parameters stayed the same.

**Thermal bonding of nanofibre mats:** For the thermal bonding experiments, the magnetic 0.2 mm thick mat was sandwiched between two non-magnetic 1.0 mm thick mats (see Fig. 3), and magnetic heating was induced in an alternating magnetic field of 25 kA/m at 400 kHz. The temperature within the magnetic layer was measured during magnetic heating by means of a fiber optic temperature sensor (FOTEMP, Optocon, Germany).

### 2.3. Characterization of magnetic nanoparticles and nanofibre mats

The crystallinity of the  $\text{Fe}_3\text{O}_4$  was characterized by XRD (D/Max-2550 PC, RIGAKU, Japan). Thermogravimetric analysis was done with approximately 10 mg of sample on a thermo-analyzer (TGA Instruments Q500, USA) at a heating rate of 10 °C/min from 30 to 600 °C under the protection of nitrogen flow. The magnetic properties of the MNPs was measured at room temperature on a vibrating sample magnetometer (VSM 7404, Lake Shore, USA) from  $-5$  kOe to 5 kOe. The morphology of the nanofibre mats was analyzed using scanning electron microscopy (SEM, Hitachi S-3000 N, Japan).

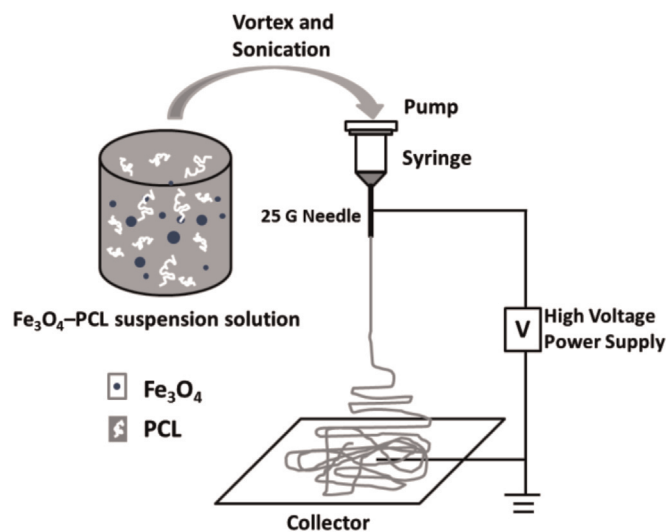


Fig. 1. Schematic of preparation and electrospinning of magnetic nanofibre mats.

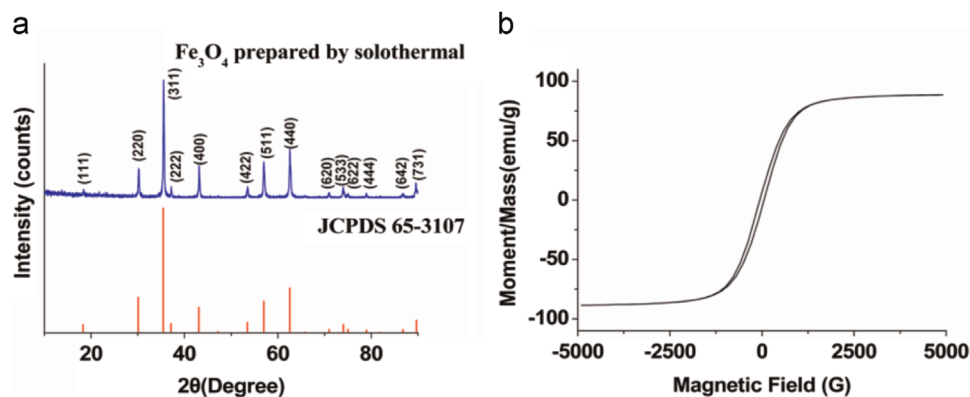


Fig. 2. (a) XRD pattern of  $\text{Fe}_3\text{O}_4$  MNPs. (b) Magnetization curve of  $\text{Fe}_3\text{O}_4$  MNPs.

### 3. Results and discussion

#### 3.1. Characterization of the $Fe_3O_4$ MNPs

XRD showed clearly (by comparison to JCPDS 65-3107) that the MNPs consisted of  $Fe_3O_4$  with high crystallinity and a cubic Fd3m

structure (Fig. 2a). The size of the MNPs was between 20 and 30 nm, as measured by transmission electron microscopy. The saturation magnetization of the hydrophilic MNPs was 88.5 emu/g and the particles showed ferrimagnetic behavior with a coercivity ( $H_C$ ) of  $\sim 80$  Oe and a relative remanence ( $M_r/M_s$ ) of 0.12 (Fig. 2b). After being attracted by a magnet, the MNPs could be easily

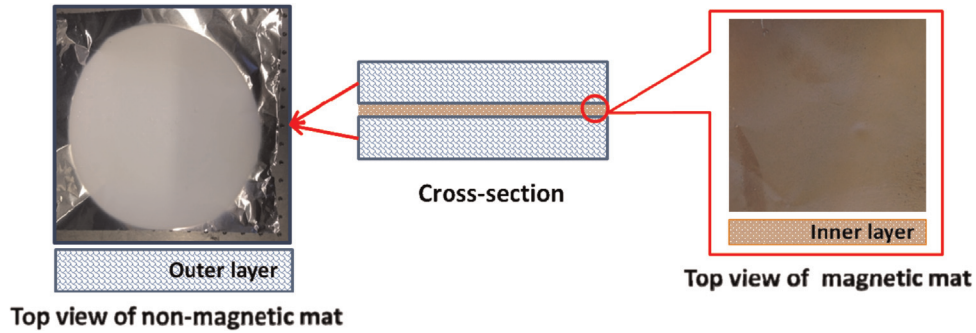


Fig. 3. Schematic of the polymer mat structure for use as a magnetically bondable material and photography of the prepared polymeric layers.

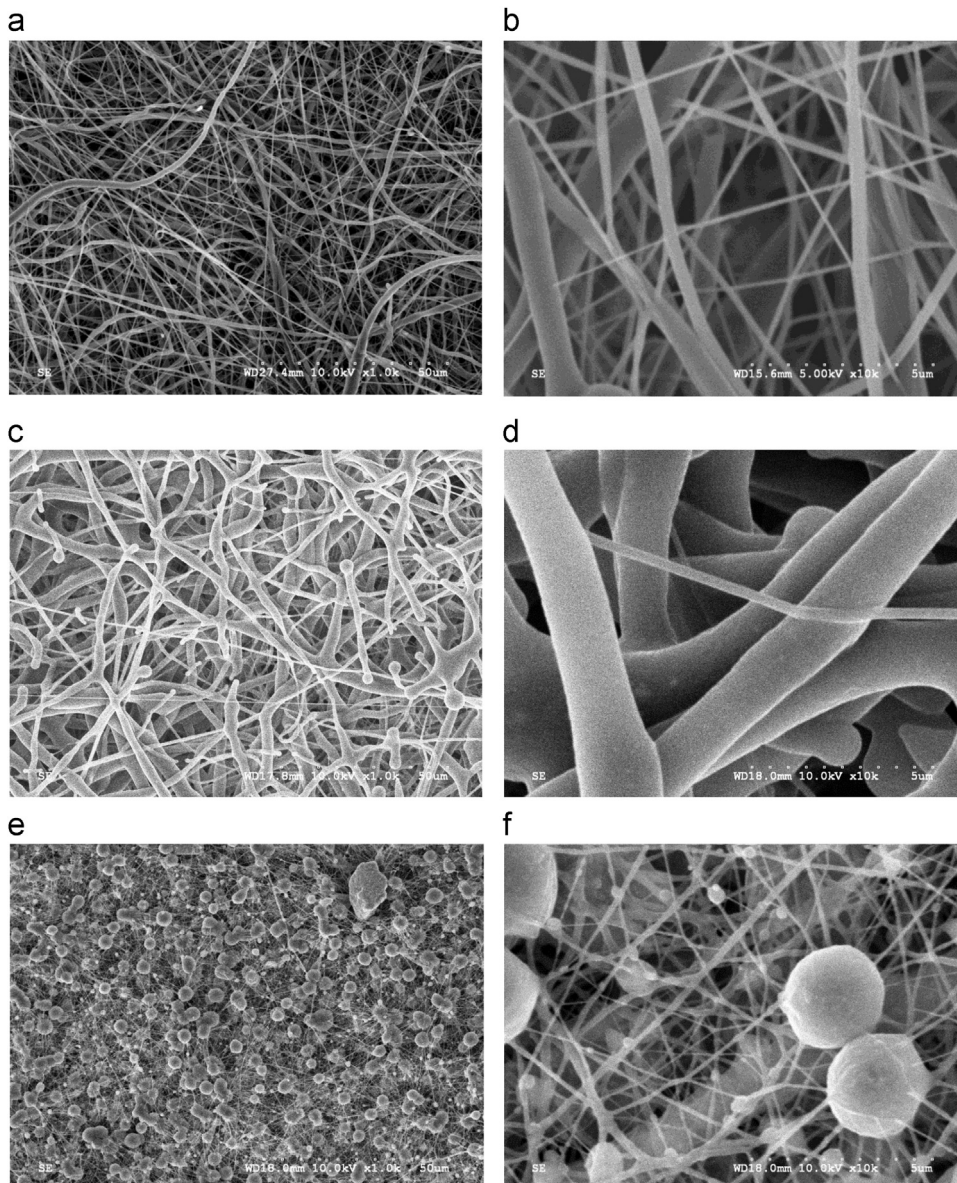


Fig. 4. SEM of electrospun PCL mats with (a, b) 0 wt% MNPs, (c, d) 19.4 wt% MNPs, and (e, f) 32.8 wt% MNPs. The magnification of (a, c, e) was 1000x and (b, d, f) 10,000x.

redispersed in methanol after light shaking. This confirms a high stability of the particles against agglomeration and sedimentation which is a basic requirement for a homogeneous dispersion of the particles within the fibers and mats.

### 3.2. Morphology of the magnetic nanofibre mats

Fig. 3 illustrates the concept of a magnetic nanofibre sandwich structure. Macroscopically, the electrospun magnetic and non-magnetic PCL mats appeared to be uniform.

The addition of 32.8 wt%  $\text{Fe}_3\text{O}_4$  MNPs to the polymer changed the microscopic morphology of the fibers from well-defined fibers with a diameter between 100 and 1000 nm (Fig. 4a and b) to nanofibers with extensive bead clusters (Fig. 4e and f). At an intermediate MNP concentration of 19.4 wt% (Fig. 4c and d), no bead formation was observed.

It seems that only higher MNP contents alter the structure of the electrospun nanofibers, as the nanofibers with 19.4 wt% MNP are almost indistinguishable from non-MNP containing nanofibers. For all of the magnetic nanofibers that we prepared, the MNPs were homogeneously incorporated into the polymer fibers. This is very different from the recently reported magnetic polyurethane fibers [21], where the MNPs tended to adhere to the polymer surface. However, no quantitative analysis of the homogeneity of MNP distribution throughout the nanofibers has been conducted.

### 3.3. Thermoanalysis of the magnetic PCL nanofibre mats

The content of  $\text{Fe}_3\text{O}_4$  in the PCL mats was confirmed by TGA. As shown in Fig. 5, there is a distinct weight loss from 240 °C to 350 °C caused by the degradation of PCL. At degradation temperature, the molecular chains of PCL decomposed to  $\text{CO}$ ,  $\text{CO}_2$  and  $\text{H}_2\text{O}$ . As these vapors escaped from the sample chamber, weight loss was sensed and recorded. Since MNPs did not undergo degradation, the weight of MNPs was recorded as the residual weight and stayed constant upon further heating. Hence the mass fraction of  $\text{Fe}_3\text{O}_4$  was determined to be about 19.4% and 32.8%, which is consistent with the amount of MNPs used to prepare the electrospinning suspension.

### 3.4. Magnetic heating of the magnetic nanofibre mats

Fiber optic measurements showed a fast increase in temperature from room temperature to above 90 °C within 40 s (see Fig. 6).

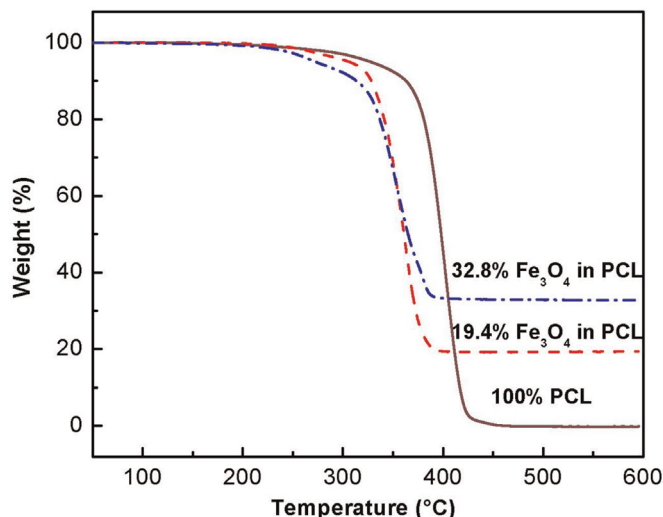


Fig. 5. TGA of PCL and magnetic nanofibre mats.

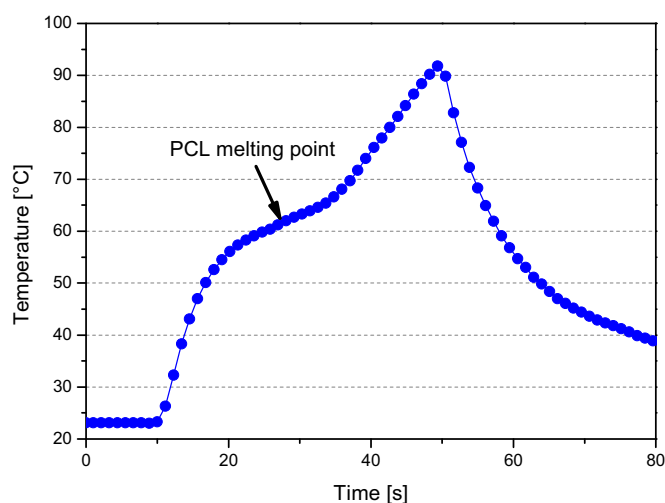
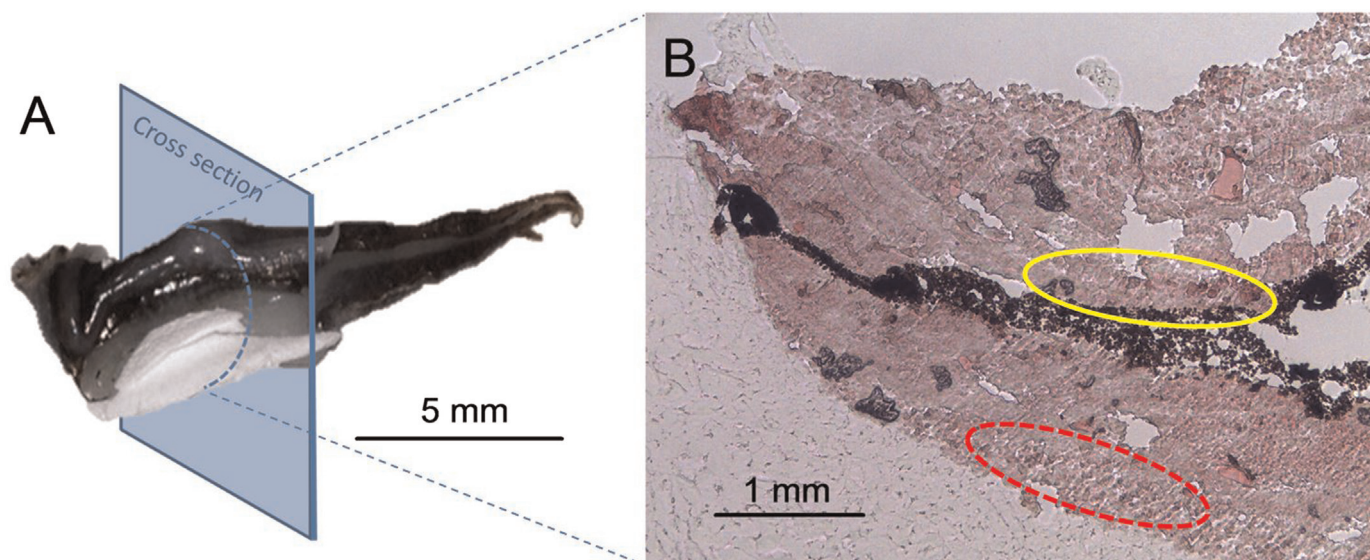


Fig. 6. Heating curve of the combination magnetic and non-magnetic PCL nanofibre mats. The alternating magnetic field was switched on 10 s after beginning of the temperature measurements and switched off 40 s later. The arrow indicates melting of PCL at about 61 °C.

This led to complete melting of the magnetic mat between the non-magnetic mats, as shown by the change of the mat's external look (compare Fig. 3 to Fig. 7a). A microscopic look at the cross section of the fused mats (Fig. 7b) showed that the polymer fibers close to the MNP mat (yellow) were molten solid, but not the nanofibers farther away (red). Magnetic heating thus very specifically heats the polymer mat with the MNPs, plus an area surrounding it of approximately 0.2–0.5 mm within the short heating time used. The precise melting of a predetermined region is thus possible in a predictable way, although it might be necessary to take into account the heat conducting properties of the polymer layers.

The energy necessary to melt a 98 mg heavy mat at 61 °C ( $\Delta T = 38$  K) was calculated from an assumed specific heat capacity similar to that of PCL of 1700 J/(K kg) for the complete sandwich to be about 7 J. Taking into account that it took 20 s to increase the temperature to the polymer's melting temperature (Fig. 6), an overall heating power of all particles within the mat of 0.35 W results. Normalizing this heating power to the mass of the magnetic layer in the center of the sandwich or the mass of the complete sandwich leads to a specific heating power of 40 W/g for the magnetic layer and about 3.5 W/g for the complete sandwich. The heating power of the magnetic heating layer should thus be sufficient to fuse mats under more realistic conditions, where contributions of heat dissipation to the surrounding area must be taken into account.

Depending on particle size and strength of particle fixation to the matrix, different mechanisms contribute to magnetically induced heating of magnetic nanoparticles – namely Néel relaxation, Brownian relaxation, and hysteresis [22]. Since particles are incorporated and thus fixed in the fibers, a completed rotation of the particles (extrinsic relaxation) can be excluded and so no contribution of Brown losses to magnetic heating takes place. For fixed particles only Néel losses and hysteresis losses are responsible for magnetic reversal loss heating. From the hysteresis curve of the particles a coercivity of about 80 Oe and a relative remanence of 0.12 was determined. These values are a clear indication for dominating ferrimagnetic behavior of the particle inside the fibers and thus hysteresis will be the main loss mechanism during magnetization reversal. Due to the particle size distribution there will also be a fraction of very small superparamagnetic particles present within the particle ensemble which flip their magnetization by means of Néel relaxation.



**Fig. 7.** Melted together magnetic and non-magnetic PCL nanofibre mats. (a) Optical image with a dotted line indicating where (b) a microscopic cross section was taken. The polymer fibers close to the MNP mat (yellow) are molten solid, but not the nanofibers farther away (red). The dark line going from left to right is the MNP-containing mat that became fused to the non-magnetic mats above and below. (For interpretation of the references to color in this figure legend, the reader is referred to the web version of this article.)

For temperature measurement the sample was folded to a small cube and the temperature probe was placed inside. For a better heat coupling from mat to sensor a drop of oil was used as thermal bridge. This certainly distorts the thermal properties of the mat but enables a reliable measurement of temperature in such small dry samples. The thermal properties of the oil drop were neglected in all heating calculations. Furthermore, the probe has a heat capacity which was not included in thermal estimations. Our experiment clearly shows that non-contactless temperature measurements on the microscale are challenging and will lead to an underestimation of the real heating power of the magnetic mats.

#### 4. Conclusions

We report here the fabrication and characterization of electro-spun magnetite nanofibre mats with good heating properties in an alternating magnetic field. We specifically demonstrated a material design concept where magnetic nanoparticles embedded in polymeric nanofibres can be used to melt a surrounding polymer from within and thus use a thin inner magnetic polymer mat to seal two non-magnetic polymer mats together, without the need of any binding agent or surfactant. In this method, even pressure sensitive polymer structures (which would lose their initial structure upon being pressed together with the commonly used heated plate method) or materials that degrade when heated throughout can be joined. The prepared mats are biocompatible and biodegradable, as all parts such as PCL and MNPs are non-toxic [20,23]. Furthermore, the nanostructure of the non-magnetic polymer more than 0.5 mm away from the magnetic mat still consisted of non-melted nanofibres. The heat seal appears to be strong, but further testing must be conducted to confirm this. The effect of the MNPs size and size distribution, and its optimal particle concentration in the nanofibre mat will have to be further studied and optimized.

The magnetic hyperthermia induced heat sealing system could also be applied easily in *in vivo* clinical applications, for example in magnetic hyperthermia treatments of cancer, as coatings on medical devices (e.g., stents) and implants, and in combination with nanofibre-encapsulated drugs as a drug delivery system

which releases the drugs upon local, internal heating. Other more technical heat sealing applications are also possible where a piece of material can be heated just where needed, thus preventing heat-induced stress and aging of sensitive parts. This might also be important in the creation of biological structures even while heat-sensitive materials, proteins and cells are present.

#### Acknowledgments

The authors gratefully acknowledge the support of Discovery Grant and CFI by the Natural Sciences and Engineering Research Council of Canada (NSERC) in Canada and the Central Universities of China Ministry of Education (Item no. 2013D110525) for their financial support to complete this work.

#### References

- [1] S. Dutz, R. Hergt, *Int. J. Hypertherm.* 29 (2013) 790.
- [2] C.L. Dennis, R. Ivkov, *Int. J. Hypertherm.* 29 (2013) 715.
- [3] A. Jordan, R. Scholz, P. Wust, et al., *Int. J. Hypertherm.* 13 (1997) 587.
- [4] I. Hilger, W. Andra, R. Hergt, et al., *Radiology* 218 (2001) 570.
- [5] B. Kozissnik, A.C. Bohorquez, J. Dobson, et al., *Int. J. Hypertherm.* 29 (2013) 706.
- [6] K.M. Krishnan, *IEEE Trans. Magn.* 46 (2010) 2523.
- [7] A.B. Salunkhe, V.M. Khot, S.H. Pawar, *Curr. Top. Med. Chem.* 14 (2014) 572.
- [8] D. Ortega, Q.A. Pankhurst, in: P.C.O'Brien (Ed.), *Nanoscience*. Royal Society of Chemistry, Cambridge, p. 60, 2013.
- [9] W. Andrä, U.O. Häfeli, r. Hergt, et al. *Novel materials*. In: h. Kronmüller, S. Parkin (Eds.), *The Handbook of Magnetism and Advanced Magnetic Materials*, vol. 4, John Wiley & Sons Ltd., Chichester, UK, 2536 p., 2007.
- [10] A.K. Gupta, M. Gupta, *Biomaterials* 26 (2005) 3995.
- [11] N. Tran, T.J. Webster, *J. Mater. Chem.* 20 (2010) 8760.
- [12] A.P. Khandhar, R.M. Ferguson, J.A. Simon, et al., *J. Biomed. Mater. Res. A* 100 (2012) 728.
- [13] C. Rumenapp, B. Gleich, A. Haase, *Pharm. Res.* 29 (2012) 1165.
- [14] A. Tomitaka, T. Koshi, S. Hatsugai, et al., *J. Magn. Magn. Mater.* 323 (2011) 1398.
- [15] K.F. Ko, Y. Li, L. Lin, et al., *J. Fiber Bioeng. Inform.* 6 (2013) 129.
- [16] T.J. Sill, H.A. von Recum, *Biomaterials* 29 (2008) 1989.
- [17] D.S. Katti, K.W. Robinson, F.K. Ko, et al., *J. Biomed. Mater. Res. B: Appl. Biomater.* 70 (2004) 286.
- [18] F. Ko, Y. Gogotsi, A. Ali, et al., *Adv. Mater.* 15 (2003) 1161.
- [19] S. Dutz, M. Kettering, I. Hilger, et al., *Nanotechnology* 22 (2011) 265102.
- [20] H. Deng, X. Li, Q. Peng, et al., *Angew. Chem. Int. Ed. Engl.* 44 (2005) 2782.
- [21] A. Amarjargal, L.D. Tijing, C.-H. Park, et al., *Eur. Polym. J.* 49 (2013) 3796.
- [22] R. Muller, R. Hergt, S. Dutz, et al., *J. Phys. - Condens. Matter* 18 (2006) S2527.
- [23] M. Kallrot, U. Edlund, A.C. Albertsson, *Biomaterials* 27 (2006) 1788.